Desalination and Water Treatment
www.deswater.com
doi: 10.5004/dwt.2022.28563

264 (2022) 259–269
July

A tailored metal–organic framework applicable at natural pH for the removal of 17α-ethinylestradiol from surface water

Parisa Javidan, Majid Baghdadi*, Ali Torabian, Behnoush Aminzadeh Goharrizi

School of Environment, College of Engineering, University of Tehran, 1417853111, Tehran, Iran,
Tel. +98 21 61113171, Fax: +98 21 66407719; emails: m.baghdadi@ut.ac.ir (M. Baghdadi) ORCID 0000-0001-9816-764X,
p.javidan71@ut.ac.ir (P. Javidan), atorabi@ut.ac.ir (A. Torabian), bamin@ut.ac.ir (B.A. Goharrizi)

Received 6 November 2021; Accepted 9 May 2022

ABSTRACT

The use of metal–organic frameworks as efficient adsorbents for micropollutants removal has attracted significant interest recently, while the effect of linkers on their performance was not examined extensively. The present paper was devoted to examining the removal of 17α-ethinylestradiol (EE2), a synthetic hormone with high-potency estrogenic contamination, from surface water by adsorption process using MIL-53(Fe) and NH_2-MIL-53(Fe) as metal–organic frameworks adsorbents constructed with different linkers. Batch experiments were designed using the Design-Expert software by considering the effective parameters, including the initial concentration of EE2, adsorbent dosage, and pH. The effects of total dissolved solids and temperature were investigated as well. The adsorbent synthesis was done by the solvothermal method, and field-emission scanning electron microscopy, X-ray diffraction, Fourier-transform infrared spectroscopy, Brunauer–Emmett–Teller, and energy-dispersive X-ray spectroscopy analyses were performed to evaluate the characterization of the prepared adsorbent. The results of characterizations showed the crystalline structure of NH_2-MIL-53(Fe) with a high specific surface area of 743 m^2/g. According to the preliminary tests, NH_2-MIL-53(Fe) was more efficient than MIL-53(Fe), especially in natural waters with neutral pH. In the case of using 2-aminoterephthalic acid as a linker, in addition to Van der Waals attraction, electrostatic interaction is involved in the adsorption of EE2 and improves removal efficiency. The easy regeneration and reusability of NH_2-MIL-53(Fe) for several cycles make it suitable for EE2 removal in natural water resources.

Keywords: Endocrine-disrupting chemicals; 17α-ethinylestradiol; Metal–organic frameworks; Adsorption; Surface water

1. Introduction

Water quality is directly related to human health and living organisms. Over the years, various pollutants, including organic and various chemical contaminants in water, have been identified, and their effects on human health have been studied. In recent years, micropollutants have attracted the attention of researchers because they are far more harmful than some other pollutants [1,2]. Pharmaceuticals and personal care products (PPCPs), and endocrine disruptors are groups of organic contaminants that have been identified in waters around the world [3]. Meanwhile, endocrine disruptors have received more attention from law enforcement agencies due to the possible high exposure to these substances and their dangerous effects on human and wildlife health, although they exist at low concentrations [1,4–6].

Among these compounds, 17α-ethinylestradiol (EE2), a synthetic estrogen, is widely used in birth control pills and drugs aimed at treating hormonal diseases. According to several studies, EE2 is more resistant to biological degradation than other similar natural hormones, thereby

* Corresponding author.

having a much longer half-life than natural hormones [7]. This means that it does not tend to decompose in nature, so living organisms are much more likely to be suffered from exposure to this particular hormone. As a result, EE2 is classified as a high-risk pollutant for humans and fish [8–10]. Adverse effects of this endocrine disruptor on humans include decreased sperm count, infertility, increased breast disease, testicular, prostate, and cervical cancer [11–13].

In general, various biological, physical, and chemical processes, such as the adsorption process, are used to remove EE2 [14–17]. The research showed the inefficiency of the biological and some physical processes in removing EE2; for example, Damkjaer et al. [8] examined EE2 amounts in the influent and effluent of two stabilization ponds of wastewater treatment systems in Morogoro, Tanzania and indicated these amounts could pose a high risk of interfering with the normal function of the endocrine systems of fish and wildlife, thereby causing an adverse impact on their reproduction and population. Mohagheghian et al. [18] studied EE2 and some other hormones in raw sewage influent and final treated effluent of seven wastewater treatment plants in Tehran, Iran in two seasons (summer–autumn), and the result showed that the mean removal efficiency of EE2 was about 80%. Also, Silva et al. [15] investigated membrane separation to eliminate mentioned contaminant, establishing the best result of 57% for EE2 removal. Furthermore, the formation of byproducts, which are sometimes more dangerous than the primary contaminant, has been reported in chemical processes [19–21]. Moriyama et al. [22] investigated the chlorination by-products of EE2, showing some of them are more dangerous than the primary contaminant.

The adsorption process has attracted the attention of researchers because of the possibility of regenerating and tailoring the adsorbents with highly selective interactions [23]. Kent and Tay [14] examined the adsorption and degradation process in an aerobic granular sludge sequencing batch reactor, concluding that the main removal mechanism for EE2 was adsorption with an average removal efficiency of 77%.

Some of the common adsorbents, such as activated carbon and anthracite were used for adsorptive removal of EE2 in previous research and their adsorption capacities were reported to be about 0.4 and 0.3 mg/g, respectively [24–26]. In this regard, the use of nanoparticles in the removal of contaminants in water and wastewater has gained a lot of attention due to the high adsorption capacity. Metal–organic frameworks (MOFs) are nanostructures with unique features such as very high surface area and porosity, uniform and ultra-regular pore size, a high degree of design capability, easy synthesis conditions, and maintaining the integrity of the flexible structure after adsorption or withdrawal of guest molecules. MOFs are constructed of metal clusters and organic linkers, which are connected via coordination bonds and form a uniform and porous crystalline structures [27–30]. Abazari et al. [31] and Azhar et al. [32] investigated the efficiency of metal–organic frameworks for antibiotics (amoxicillin, ampicillin, cloxacillin, and sulfachlorpyridazine) removal, resulting in approximately 90% removal efficiency.

In this research, two MOFs were synthesized using iron(III) cations as the core coordinated adsorbent with terephthalic acid and 2-aminoterephthalic acid as ligands. It is expected that the type of the linker in the MOF structure could be effective in the interactions involved in the adsorption process, especially at neutral pH. Using the adsorption process as a high-efficient and innovative approach for removing EE2 with leaving no trace of dangerous by-products was investigated in the presence of mentioned MOFs as adsorbents. Because the linkers significantly impact the efficiency of adsorption by MOF, different linkers were explored to select the suitable one for removing EE2 at natural pH. The applied adsorbents in this study, especially NH_2-MIL-53(Fe), are known as selective adsorbents with porous structure and high stability, making them effective in EE2 elimination from aquatic environments. The prepared adsorbent was identified by characterization tests, including scanning electron microscopy, Fourier-transform infrared spectroscopy (FTIR), X-ray diffraction (XRD), Brunauer–Emmett–Teller (BET), and energy-dispersive X-ray spectroscopy (EDS) analysis. The central composite design (CCD) and the response surface methodology (RSM) were applied simultaneously for the determination of effective parameters in batch adsorption experiments, such as pH, adsorbent dosage, and initial concentration of EE2. More examinations of the adsorption process were accomplished by investigation of isotherm and thermodynamic parameters. Finally, the regeneration capability of the adsorbent was checked in several cycles.

2. Materials and methods

2.1. Materials

EE2 ($C_{20}H_{24}O_2$) was purchased as a white, odorless solid crystalline powder from the Iran Hormone Pharmaceutical Company and was used as the contaminant for spiking in samples. The terephthalic acid ($C_8H_6O_4$), 2-aminoterephthalic acid ($HO_2C{-}C_6H_3NH_2{-}CO_2H$), $FeCl_3{\cdot}6H_2O$ (99.5%), N,N-dimethylformamide (DMF, 99.8%), and methanol (99%) were used to synthesize the adsorbent. The pH adjustment was performed using HCl and NaOH solutions (0.1 mol/L). Potassium dihydrogen phosphate (KH_2PO_4), dichloromethane (CH_2Cl_2), and acetonitrile (C_2H_3N) were supplied for the sample preparation step. All these mentioned materials and $MgSO_4$, $NaHCO_3$, KNO_3, and $CaCl_2$ for the preparation of total dissolved solids (TDS) solutions were purchased from Merck (Darmstadt, Germany) except 2-aminoterephthalic acid, which was purchased from Sigma-Aldrich (Taufkirchen, Germany), and all of them were used without further purification.

2.2. Synthesis of the adsorbents

In this research, the solvothermal method was used to synthesize MOFs [33,34]. In brief, NH_2-MIL-53(Fe) was synthesized using a solution containing $FeCl_3{\cdot}6H_2O$, 2-aminoterephthalic acid (NH_2-BDC), and N,N-dimethylformamide with a molar ratio of 1:1:280 ($FeCl_3{\cdot}6H_2O$:NH_2-BDC:DMF) was prepared. For this purpose, 1 g (3.7 mmol) of $FeCl_3{\cdot}6H_2O$ and 0.67 g (3.7 mmol) of 2-aminoterephthalic

acid were dissolved in 80 mL (1,033 mmol) of N,N-dimethylformamide. In the next step, the prepared solution was placed in an autoclave for 17 h at 145°C. After cooling the solution at ambient temperature, the obtained MOF was washed with N,N-dimethylformamide and methanol and centrifuged at 5,000 rpm several times to remove residuals. Finally, it was dried for 12 h at 70°C [35–37]. It should be noted that for MIL-53(Fe) preparation, the type of linker was only changed, and the materials were combined with the same molar ratio.

2.3. Characterization of the adsorbent

A field-emission scanning electron microscope (FE-SEM, MIRA3, TESCAN, Czech Republic) was used to determine the morphological characteristics of the adsorbent. Fourier-transform infrared spectrum (FTIR Spectrum RX I, PerkinElmer, USA) was applied for the identification of the surface functional groups of the adsorbent in the range of 400–4,000 cm^{-1}. Brunauer–Emmett–Teller (BET, BELSORP mini II, Japan) was employed for evaluating the pore diameters, pore volumes, and specific surface area of the synthesized adsorbent. X-ray diffraction patterns were recorded at $1° < 2\theta < 80°$ to investigate the crystal structure of MOFs using (XRD, X'Pert PRO MPD, PANalytical, Netherland). Energy-dispersive X-ray spectroscopy (EDS, Oxford Detector, England) was utilized to investigate the elemental content of the adsorbent.

2.4. Experimental design and data analysis

Batch experiments were used for EE2 adsorption in this research. Effective parameters and their ranges were determined based on the pre-tests. The experiments were designed by Design-Expert 10 (Stat-Ease Inc., Minneapolis, United States) for the optimization of the adsorption process based on the Box–Behnken Design and RSM. The removal efficiency as the response depends on pH, adsorbent dosage (mg/L), and initial concentration of EE2 (μg/L), which are labeled as *A*, *B*, and *C*, respectively (Table 1).

The total number of the designed experiments was 17 runs and the assessment of experimental errors was controlled via 5 center points, as shown in Table 2. The adequacy of the quadratic model and correlation between variables and the significance of each one was evaluated by the analysis of variance (ANOVA). The role of the three main factors (pH, adsorbent dosage, and initial concentration) on the removal of EE2 and their interactions were presented by the 3D response surface plots. Due to the presence of inorganic ions in real water samples, the adsorbent performance was studied in the presence of other ions by designing and performing a series of experiments. For this purpose, a solution containing inorganic salts with a final TDS of 2,000 mg/L was prepared as the TDS stock solution, and it was used to prepare the samples with different TDS levels. The saturated adsorbent was placed in 15 mL of methanol and shaken for 5 min to determine the number of regeneration cycles for the adsorbent. Because of the high solubility of EE2 in methanol, the adsorbed EE2 can be released in methanol, thereby resulting in recovered adsorbent with free active sites. The adsorption/desorption cycle continued until a significant downward trend in the adsorption capacity of the adsorbent was observed.

Table 1
Experimental levels and ranges of effective parameters for EE2 adsorption

Factors	Unit	Levels		
		–1	0	+1
A: pH	–	4.5	7	9
B: Adsorbent dosage	mg/L	100	250	400
C: Initial concentration	μg/L	50	275	500

2.5. Analytical methods

After performing the adsorption process, the samples were concentrated by liquid–liquid extraction and filtered with PTFE syringe filters (0.2 μm). The residual concentration of EE2 was determined using high-performance liquid chromatography (HPLC, Agilent 1100, Santa Clara, United States), supplemented with a C18 column (5 μm, 4.6 mm × 150 mm) and a UV detector set at 205 nm, and an isocratic elution mode with a fixed mobile phase composition. Acetonitrile/buffer (40/60) was used as the mobile phase with a flow rate of 1 mL/min [38,39]. The pHs were detected by a pH meter (Behineh B-2000, Iran), and TDS was measured by TDS/EC conductometer (Metrohm 691, Switzerland).

2.6. pH_{zpc} and ash content determination

The general procedure of pH_{zpc} determination was performed. In brief, 0.1 mol/L KCl solution was prepared in a volume of 250 mL and was divided equally into 8 flasks of 25 mL to investigate pH_{zpc}. 0.1 mol/L NaOH or HCl solutions were used to adjust the pH in the range of 3–10. In addition, 0.1 g adsorbent was introduced to each flask. The samples were shaken for 24 h, and after that, the final pH of each flask was measured after separating adsorbents from samples using a centrifuge to establish pH_{zpc}.

The ash content of the adsorbent also was determined by heating in the muffle furnace. 1 g of NH_2-MIL-53(Fe) was placed in a crucible and then heated at 700°C for 12 h to determine the ash content of mentioned adsorbent, similar to previous studies [40].

3. Results and discussion

3.1. Comparison of synthesized MOFs performance for adsorptive removal of EE2

In order to determine the appropriate adsorbent for the removal of EE2, the performance of the prepared MOFs was studied at various pH values. As shown in Fig. 1a, the performance of both synthesized adsorbents significantly depends on the pH value. By increasing the pH, a significant decrease in the performance of MIL-53(Fe) was observed, thereby resulting in low removal efficiency in the pH range of 7–8.5. However, the performance of NH_2-MIL-53(Fe) in this pH range was significantly higher than

Table 2
RSM design values

Run	Factors			Response
	A: pH	*B*: Adsorbent dosage (mg/L)	*C*: Initial concentration (μg/L)	Removal efficiency (%)
1	9.5	250	500	68.1
2	4.5	250	500	80.5
3	7.0	250	275	80.3
4	4.5	250	50	0.3
5	9.5	100	275	50.1
6	4.5	100	275	55.2
7	7.0	250	275	82.6
8	7.0	400	50	39.9
9	7.0	250	275	83.4
10	7.0	100	50	0.5
11	7.0	250	275	75.8
12	7.0	400	500	89.0
13	7.0	250	275	69.4
14	7.0	400	500	92.1
15	9.5	400	275	65.2
16	4.5	400	275	85.5
17	9.5	250	500	79.8

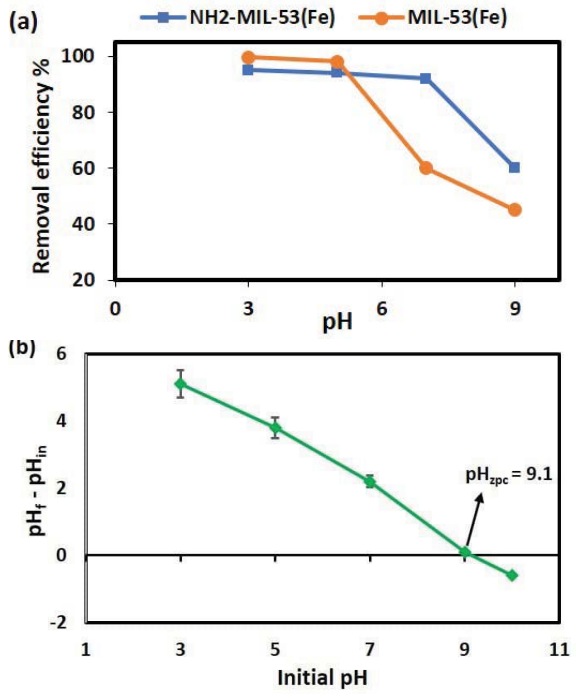

Fig. 1. (a) Comparison of the MIL-53(Fe) and NH_2-MIL-53(Fe) performance in different amounts of pH for EE2 removal and (b) pH_{zpc} determination of NH_2-MIL-53(Fe).

that of MIL-53(Fe). There are two interactions between MIL-53(Fe) and EE2, electrostatic interactions due to its active amine groups and Van der Waals forces because of aromatic rings, which significantly impact the higher adsorption capacity of the adsorbent. Positively charged amino functional groups incorporated in NH_2-MIL-53(Fe) can interact with the negatively charged functional groups of contaminants and improve removal efficiency. According to the pH of surface waters, NH_2-MIL-53(Fe) was selected as the suitable MOF for the removal of EE2 in this study. In addition to the higher adsorption capacity of NH_2-MIL-53(Fe) compared to MIL-53(Fe) at the natural pH (surface water), it also exhibits better performance in most different tested pHs, making it a better choice to apply in various environments.

Fig. 1b indicates the pH_{zpc} of NH_2-MIL-53(Fe) is equal to 9.1, according to obtained data. Therefore the adsorbent has a positive charge at neutral pH and a negative charge at alkaline pHs. This finding is consistent with the data in Fig. 1a, in which as the pH of the sample goes to alkaline ranges, the adsorption of EE2 declines due to the weakening of electrostatic interaction between adsorbent and contaminant. The ash content of NH_2-MIL-53(Fe) was also determined to be 16% of the total adsorbent mass.

3.2. Characterization of adsorbent

The morphological aspects of the adsorbent were investigated using the FE-SEM analysis (Fig. 2a–c). As can be seen, the prepared MOFs have regular, porous, and uniformly framed octagonal crystals with an average edge length of 400 nm. The porous morphology of the adsorbent verifies its high capacity to adsorb pollutants.

According to the information obtained from the corresponding EDS spectrum (Fig. 2d), as expected, the elements including Fe, O, N, and C in the regular structure of the final adsorbent were the same as the initial chemicals used for the preparation of the adsorbent. As shown in Fig. 2d, the amount of major elements of C, N, and O (49.45%, 10.6%,

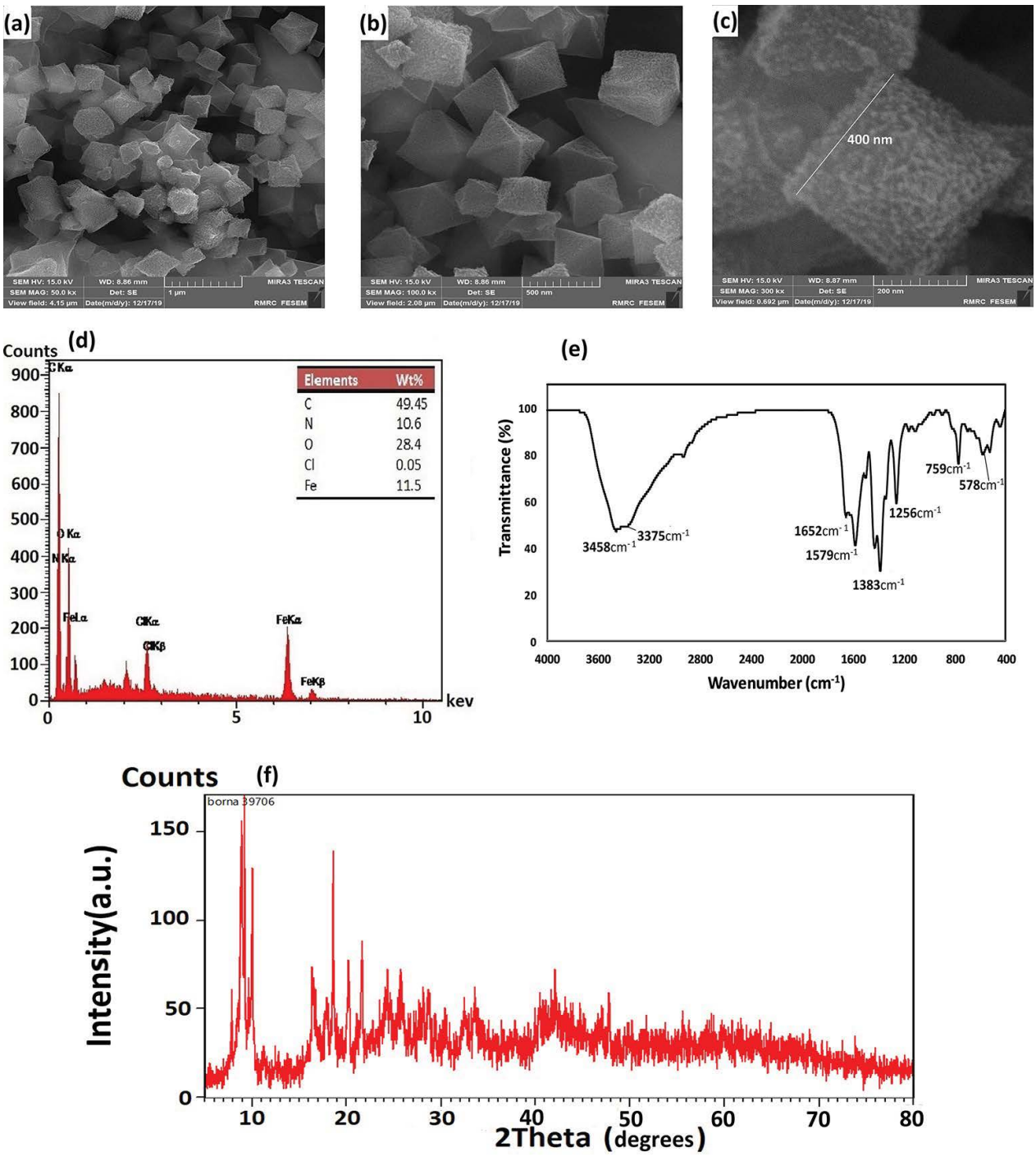

Fig. 2. FE-SEM images of NH_2-MIL-53(Fe) on different scales: (a) 1 μm, (b) 500 nm, (c) 200 nm, (d) corresponding EDS spectrum and elemental composition of NH_2-MIL-53(Fe), (e) FTIR, and (f) XRD spectra of NH_2-MIL-53(Fe).

and 28.4%, respectively) is well-matched with that reported in previous research [41]. In addition, 11.5% of the iron in the final structure proves the presence of iron clusters in the adsorbent.

The crystallographic structure and phase purity of the synthesized sample was corroborated by the XRD pattern presented in Fig. 2f. The adsorbent represents a specified crystal structure that authenticated FE-SEM results. Furthermore, the main diffraction peaks are according to the previously reported data in the literature. Meanwhile, no other peaks were detected, demonstrating the pure phase of NH_2-MIL-53(Fe) [27,41,42].

In order to further identify different chemical bonds and functional groups in the prepared adsorbent, an FTIR analysis was conducted (Fig. 2e). At about 3,458 and 3,375 cm^{-1}, the wide peaks respectively are related to the

asymmetrical and symmetrical stretching vibrations of the N–H bond, while the peak at 1,652 cm^{-1} presents bending vibrations of the N–H bond, emphasizing the presence of amino groups in the synthesized adsorbent. The two strong peaks at 1,579 and 1,383 cm^{-1} are correlated to the asymmetric and symmetric stretching vibrations of carboxyl groups in aminoterephthalic acid. In addition, the peaks at 1,256 and 1,386 cm^{-1} also refer to the C–N stretching bond, which is due to the presence of aromatic amines. Furthermore, the peaks at 759 and 573 cm^{-1} can be dedicated to the C–H bending vibrations of the aromatic ring and the Fe–O vibration bond, respectively. It is worth noting that all available peaks, as expected, were in full compliance with those reported for the synthesized MOFs with iron cores, establishing that the synthesis of adsorbent has been performed successfully [27,41,43].

BET method is the most well-known procedure used to assess the surface area of MOFs. According to BET results, the specific surface area of the adsorbent was 743 m^2/g, which is a hundred times higher than that of some other MOFs; for example, Yılmaz et al. [44] reported 23 m^2/g for the specific surface area of MIL-53(Fe). Also, the average diameter of the adsorbent pores is 2.4 nm, which confirms the microporous structure of the adsorbent and illustrates its suitability for trapping the target micropollutant. Also, the pore volume of the synthesized NH_2-MIL-53(Fe) is 0.45 cm^3/g, which is larger than the pore volume of activated carbon (0.215 cm^3/g) or graphene nanosheets reported (0.1–0.18 cm^3/g) in previous research [45,46].

3.3. Effect of pH, adsorbent dosage, and initial concentration of EE2

As mentioned earlier, *A* (pH), *B* (adsorbent dosage), and *C* (initial concentration of contaminant) were considered the effective parameters, and the following equation, which has been acquired from the Design-Expert software, demonstrates the correlation between *A*, *B*, and *C* and removal efficiency as the response obtained by the software.

$$\begin{aligned}\text{Removal} = &-189.73 + 41.38A + 0.20B + 0.56C \\ &- 0.010AB - 0.01AC - 0.01BC \\ &- 2.84A^2 + 0.01B^2 - 0.01C^2\end{aligned} \quad (1)$$

The ANOVA results are shown in Table 3. The *p*-values less than 0.05 indicate the significant effect of the chosen factors on the removal performance. The effect of pH, adsorbent dosage, and initial concentration of EE2, as well as the interaction of pH and adsorbent dosage, were significant (*p*-value > 0.05). The *p*-value and *F*-value of the model indicate that only 0.01% of the model matching may have occurred randomly. Additionally, no significant lack of fit confirmed the validity of the model. On the other hand, R^2-values are defined as correlation coefficients and describe the consistency between the calculated and experimental data and also the difference between the predicted determination coefficient (Pred. R^2) and adjusted determination coefficient (Adj. R^2) was about 0.2, which indicates the model precision. Eventually, the amount of Adeq. precision was much more than 4, which is an appropriate feature.

The predicted data obtained from Eq. (1) were plotted against actual data (Fig. 3a). As can be seen, all results are close to the experimental data with no significant deviation, which proves an excellent correlation between the proposed model and experimental results. Also, as can be seen in Fig. 3b, the normal plot of residuals exhibit linear behavior and constant distribution, confirming the accuracy of the assumption of normality.

The perturbation plot is shown in Fig. 3c and displays the effect of all parameters in one plot by shifting one parameter in a specified range while keeping other factors constant. The vertical axis is associated with the removal efficiency, whereas the horizontal axis shows the 3 levels of independent variables. A high slope for a parameter is a

Table 3
Analysis of variance (ANOVA) for the response surface quadratic model for EE2 removal

Factor	Sum of square	Degree of freedom	Mean square	*F*-value	*p*-value	
Model	15,933.50	9	1,770.39	164.69	<0.0001	Significant
A: pH	171.13	1	171.13	15.92	0.0072	
B: Adsorbent dosage	820.13	1	820.13	76.29	0.0001	
C: Initial concentration	10,512.50	1	10,512.50	977.91	<0.0001	
AB	56.25	1	56.25	5.23	0.0622	
AC	36.00	1	36.00	3.35	0.1170	
BC	441.00	1	441.00	41.02	0.0007	
A^2	1,190.25	1	1,190.25	110.72	<0.0001	
B^2	2.25	1	2.25	0.21	0.6634	
C^2	2,704.00	1	2,704.00	251.53	<0.0001	
Residual	64.50	6	10.75			
Lack of fit	35.75	3	11.92	2.28	0.4310	Not significant
Pure error	28.75	3	9.58			
Cor. total	15,998.00	15				

R^2 = 0.9960, Adjusted R^2 = 0.9899, Predicted R^2 = 0.9611, Adeq. Precision = 36.072

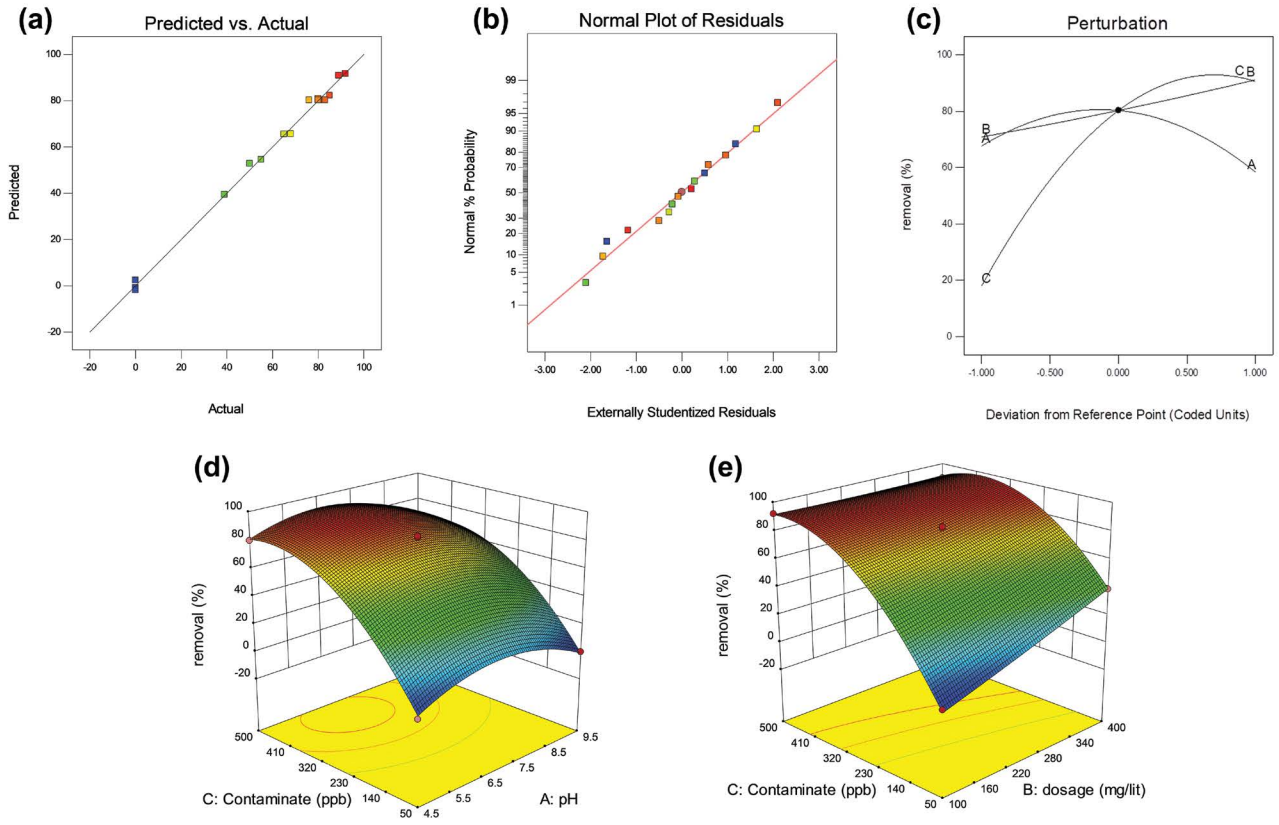

Fig. 3. (a) Predicted against actual response values, (b) normal plot of residuals for the model, (c) deviation from the reference point, and 3D response surface plots indicating the interactive impact of (d) pH and EE2 concentration and (e) dosage of adsorbent and EE2 concentration.

sign of high sensitivity of the result to this parameter, so the initial concentration of EE2 is a much more critical factor than other parameters. At first, the slope is sharp and when the concentration increase, decreasing slope confirms that its effect on removal efficiency declines. Also, the pH graph indicates a positive slope in acidic regions and a negative slope in alkaline regions. The maximum removal occurred at neutral pH, thereby making the adsorbent application practical in real water samples (pH of real water sample: 7.1). As can be clearly seen in Fig. 3d, at low pH and high EE2 concentrations, the adsorption operation is performed with much greater efficiency, but at higher pH, the effect of the pollutant concentration is decreased. These results are quite similar to previous reports and despite a large number of MOFs whose active pH range is narrow, NH_2-MIL-53(Fe) can remove EE2 in a wide pH range and show its best application in neutral pH [44,47]. Also, as indicated in Fig. 3e, the high initial concentration of the contaminant and adsorbent dosage are much better conditions for adsorbing EE2 using NH_2-MIL-53(Fe) because more adsorbent dosage provides more surface area and more active sites leading to a more effective interactions with additional EE2 and enhanced removal efficiency [44,47]. According to the three-dimensional graphs, it was found that the best conditions for removing EE2 are neutral pH and an adsorbent dosage of 400 mg/L. The validation of the proposed model also was conducted in the point prediction of Design-Expert, where it was established that the mean removal of EE2 according to designed experiments is 74%. The point prediction also showed the EE2 removal efficiency is in the range of 70% to 79% (77%).

3.4. Effect of TDS on removal efficiency of EE2

The drinking water in different areas has different values of TDS (up to 1,200 mg/L), which may affect the adsorbent behavior in the adsorption process, so the effect of TDS on the adsorption process was investigated. Therefore, the samples with the optimal conditions mentioned earlier were prepared, and their TDS concentrations were adjusted at 0, 250, 500, and 1,000 mg/L using a TDS stock solution with a composition presented in Table 4. After separating the adsorbent and sample preparation, the concentration of EE2 remaining in the solution was determined by HPLC. It should be considered that in the absence of TDS, the removal efficiency of EE2 was about 90%. As shown in Fig. 4, the removal efficiency increased with increasing TDS, which can result from the salting-out effect, thereby decreasing the water solubility of EE2, which is consistent with the results observed in previous studies [48]. Existing

aromatic rings in the proposed adsorbent cause the hydrophobic interaction between adsorbent and contaminant and result in adsorbing EE2. The higher TDS of a sample can decline EE2 solubility, enhancing the hydrophobic interaction between adsorbent and adsorbate and subsequently increasing EE2 removal efficiency. The findings indicate that synthesized adsorbent has great potential to remove the EE2 from real samples that usually contain high TDS.

3.5. Adsorption isotherms

The adsorption isotherm indicates the relationship between the equilibrium concentration of adsorbate on the surface of the adsorbent and in the solution. In the present study, the closest isotherms to the trend of experimental data were obtained from batch experiments at the optimum level of effective parameters. The examined models were Langmuir and Freundlich, and their equations and the values of the model parameters in addition to the calculated errors, are shown in Table 5. According to the OLS (ordinary least squares) values at 298 K, which were calculated from Eq. (1), the Langmuir model is less consistent with the experimental data, thereby estimating inaccurate q_m. On the other hand, the Freundlich model has less OLS and is more consistent with the predicted results, which is according to the reported results [49]. The amount of Langmuir constant (b) indicates the adsorption constant, which is related to the interaction between adsorbent and adsorbate. In the Freundlich model, more n_F expresses the more strong interaction between the adsorbent and the pollutant. In this research, the value of $1/n_F$ is equal to 1.22, which indicates favorable adsorption. The adsorption isotherm at the temperature of 298 and 323 K was investigated and the corresponding parameters are presented. It is evident that the adsorption capacity is increased at a higher temperature. However, according to OLS, the experiments at 298 K are more consistent with the calculated data from both models. Further discussions on the impact of temperature on adsorption experiments are provided in the thermodynamic section. As it is obvious, the Freundlich model exhibited less OLS at both 298 and 323 K and is more consistent to describe the experiment.

$$\mathrm{OLS} = \sum_{i=1}^{n} \left(q_{\exp} - q_{\mathrm{cal}} \right)^2 \tag{2}$$

Table 4
Composition of TDS stock solution (2,000 mg/L)

Cation	mg/L	Anion	mg/L
Ca^{2+}	235.8	SO_4^{2-}	394.2
Na^{+}	158.4	Cl^{-}	422.4
K^{+}	106.4	NO_3^{-}	169
Mg^{2+}	98.6	HCO_3^{-}	420

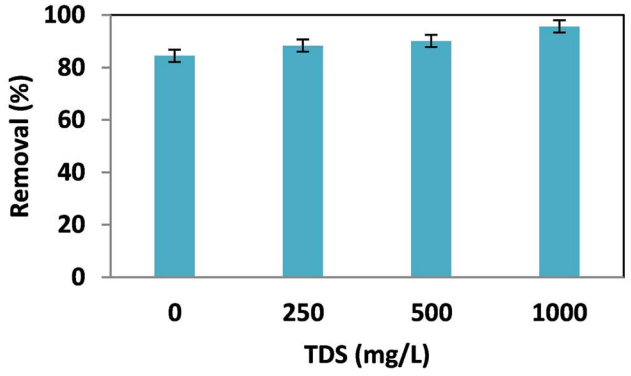

Fig. 4. TDS effect on the removal efficiency of EE2.

3.6. Adsorption thermodynamic

Another parameter affecting the rate of adsorption is temperature. In thermodynamic studies, the effect of temperature on the adsorption process is examined, resulting in thermodynamic parameters [50]. Since temperature is one of the influential factors in the removal process of EE2, its effect was investigated at 275, 283, 298, and 323 K. The experiments were performed under optimal conditions. Fig. 5 shows the plot of $\ln K_c$ vs. $1/T$ through which the thermodynamic parameters were calculated. Table 6 indicates the values of standard entropy change ($\Delta S°$ (J/mol K)), Gibbs free energy change ($\Delta G°$ (kJ/mol)), and standard enthalpy change ($\Delta H°$ (kJ/mol)), which were calculated according to Eqs. (2) and (3) using the slope and y-intercept of the diagram in Fig. 5.

$$\Delta G° = \Delta H° - T\Delta S° \tag{3}$$

$$\ln K_c = \frac{\Delta S°}{R} - \frac{\Delta H°}{RT} \tag{4}$$

where R and K_c are related to the universal gas constant (8.314 J/mol K) and the thermodynamic equilibrium constant of adsorption, respectively. Negative values of $\Delta G°$

Table 5
Parameters and values of isotherm models for EE2 adsorption

Isotherm	Equation	Value of parameter (298 K)	Value of parameter (323 K)	Calculated error
Freundlich	$\ln q_e = \ln K_f + \frac{1}{n}\ln C_e$	$1/n_F = 1.22$ K_f (mg/g)(L/mg)$^{1/n}$ = 13.7	$1/n_F = 01.03$ K_f (mg/g)(L/mg)$^{1/n}$ = 15.4	OLS = 0.0030 (298 K) OLS = 0.0034 (323 K)
Langmuir	$\frac{C_e}{q_e} = \frac{1}{bq_m} + \frac{C_e}{q_m}$	q_m (mg/g) = 5,536 b (L/mg) = 0.0016	q_m (mg/g) = 6,741 b (L/mg) = 0.0019	OLS = 0.0214 (298 K) OLS = 0.0247 (323 K)

pH: 7, adsorbent dosage: 0.4 g/L, time: 30 min

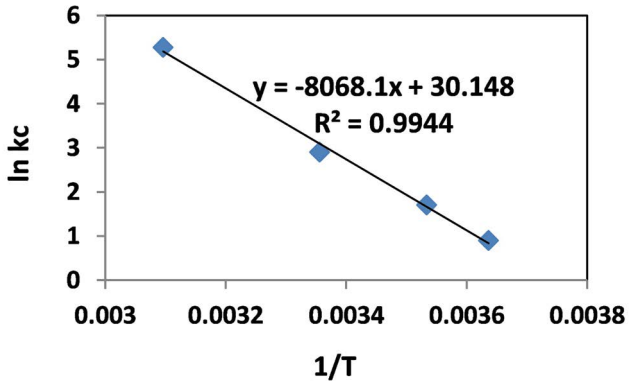

Fig. 5. Thermodynamic plot for the adsorption of EE2 (pH: 7, adsorbent dosage: 0.4 g/L, time: 30 min, EE2 concentration: 500 μg/L).

Table 6
Values of $\Delta S°$, $\Delta G°$, and $\Delta H°$

Temperature (K)	$\Delta G°$ (kJ/mol)	$\Delta S°$ (J/mol K)	$\Delta H°$ (kJ/mol)
275	–2.05	250.6	67.08
283	–4.02		
298	–7.2		
323	–14.2		

are an indication of the spontaneity of the adsorption, and the positive value of $\Delta S°$ shows that randomness at the solid–liquid interface in the adsorption process increased and also confirms that the reaction is entropy-driven. Positive values of $\Delta H°$ demonstrate that the process is naturally endothermic, which proves that the adsorption efficiency increases by increasing temperature.

3.7. Regeneration of NH_2-MIL-53(Fe) characteristics

The reusability of the adsorbent after each adsorption operation under optimal conditions was evaluated. The regeneration tests for NH_2-MIL-53(Fe) were carried out in optimum experimental conditions (adsorption: pH: 7, adsorbent dosage: 0.4 g/L, time: 5 min, EE2 concentration: 500 μg/L, temperature: 298 K; washing: methanol: 15 mL, time: 20 min). The adsorbent was separated from the sample and placed in methanol solution, which is a suitable solvent for dissolving EE2, to release the adsorbed EE2 into the methanol. The adsorption/desorption cycle continued until a significant downward trend in adsorption capacity was observed. As shown in Fig. 6, the high removal efficiency was observed in the first stage, but the efficiency decreased slightly in each cycle. The decrease in efficiency can be attributed to the binding of the pollutant at the adsorption sites, occupating active sites, as well as the loss of adsorbent amounts at the repetition of each cycle.

3.8. Comparison of NH_2-MIL-53(Fe) and other adsorbents

Compared to other common adsorbents, NH_2-MIL-53(Fe) has many advantages for EE2 removal. The synthesis process is straightforward and without using complicated

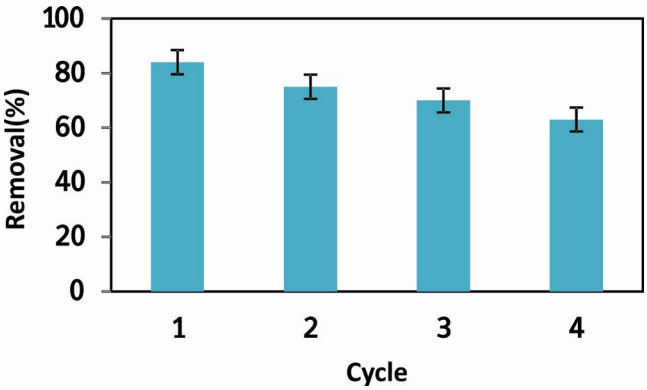

Fig. 6. Removal efficiency after each cycle of desorption experiments.

Table 7
Comparison of NH_2-MIL-53(Fe) and other common adsorbents for EE2 adsorption

Adsorbent	T (K)	pH	q_{max} (mg/g)	Reference
Powdered activated carbon	–	–	1.163	[24]
Granular activated carbon	–	–	0.436	[24]
un-anthracite	298	7	0.314	[25]
4 K anthracite	298	7	0.299	[25]
Multi-walled carbon nanotube	298	6	0.472	[51]
Magnetic graphene oxide	308	7	0.378	[52]
MIL-53(Fe)	298	7	1.26	This study
NH_2-MIL-53(Fe)	298	7	1.850	This study

instruments. The advantages include higher adsorption capacity, which is compared with other adsorbents in Table 7. This superior performance of the NH_2-MIL-53(Fe) could be because of regular and porous crystals with a high specific surface area. Furthermore, amine functional groups in the structure of NH_2-MIL-53(Fe) play an essential role in the adsorption of EE2. It can be deduced by considering operational conditions presented in Table 7 that most experiments are conducted at natural pHs and room temperature to increase the adsorbent applicability in real works. Still, the NH_2-MIL-53(Fe) indicates a higher adsorption capacity toward EE2 removal than other adsorbents reported in other studies.

4. Conclusion

In this study, for the first time, the performance of MIL-53(Fe) and NH_2-MIL-53(Fe) was investigated for the removal of EE2 as a resistant micropollutant. Compared to MIL-53(Fe), there is an electrostatic interaction advantage in addition to the Van der Waals forces in NH_2-MIL-53(Fe), which has positively charged amine functional groups, and the EE2 with the negatively charged phenolic groups. The

characterization analysis established that the porosity of the selected adsorbent and its specific surface area was high, indicating the formation of MOF crystals and suitable porous spaces for adsorbing EE2. In spite of some other MOFs, which have a narrow active pH range, NH_2-MIL-53(Fe) is an efficient adsorbent in a wide pH range and its best application is in neutral pH, making it appropriate for natural water treatment even in the presence of high amounts of TDS. According to thermodynamic studies, the adsorption process is endothermic, entropy-driven, and spontaneous. The best isotherm to interpret the adsorption process was Freundlich. Eventually, desorption experiments proved that NH_2-MIL-53(Fe) is a stable adsorbent and can be used in different adsorption cycles. Because of the different functional groups in the structure of MOFs, it can be predicted that they can be used for the adsorption of various endocrine disruptors and other perilous micropollutants.

Acknowledgments

Special thanks to the Nanotechnology Research Center of the School of Environment, College of Engineering, University of Tehran, Tehran, Iran, for supporting this research.

Declarations

The authors have no relevant financial or non-financial interests to disclose.

References

[1] M.O. Barbosa, N.F.F. Moreira, A.R. Ribeiro, M.F.R. Pereira, A.M.T. Silva, Occurrence and removal of organic micropollutants: an overview of the watch list of EU Decision 2015/495, Water Res., 94 (2016) 257–279.
[2] K.O. K'oreje, F.J. Kandie, L. Vergeynst, M.A. Abira, H. Van Langenhove, M. Okoth, K. Demeestere, Occurrence, fate and removal of pharmaceuticals, personal care products and pesticides in wastewater stabilization ponds and receiving rivers in the Nzoia Basin, Kenya, Sci. Total Environ., 637–638 (2018) 336–348.
[3] R. Tröger, P. Klöckner, L. Ahrens, K. Wiberg, Micropollutants in drinking water from source to tap - method development and application of a multiresidue screening method, Sci. Total Environ., 627 (2018) 1404–1432.
[4] C.X. Huo, P. Hickey, EDC demonstration programme in the UK – Anglian water's approach, Environ. Technol., 28 (2007) 731–741.
[5] J.P. Laurenson, R.A. Bloom, S. Page, N. Sadrieh, Ethinyl estradiol and other human pharmaceutical estrogens in the aquatic environment: a review of recent risk assessment data, AAPS J., 16 (2014) 299–310.
[6] V. Chander, B. Sharma, V. Negi, R.S. Aswal, P. Singh, R. Singh, R. Dobhal, Pharmaceutical compounds in drinking water, J. Xenobiot., 6 (2016) 5774, doi: 10.4081/xeno.2016.5774.
[7] Y. Feng, Z. Zhang, P. Gao, H. Su, Y. Yu, N. Ren, Adsorption behavior of EE2 (17α-ethinylestradiol) onto the inactivated sewage sludge: kinetics, thermodynamics and influence factors, J. Hazard. Mater., 175 (2010) 970–976.
[8] K. Damkjaer, J.J. Weisser, S.C. Msigala, R. Mdegela, B. Styrishave, Occurrence, removal and risk assessment of steroid hormones in two wastewater stabilization pond systems in Morogoro, Tanzania, Chemosphere, 212 (2018) 1142–1154.
[9] P. Schröder, B. Helmreich, B. Škrbić, M. Carballa, M. Papa, C. Pastore, Z. Emre, A. Oehmen, A. Langenhoff, M. Molinos, J. Dvarioniene, C. Huber, K.P. Tsagarakis, E. Martinez-Lopez, S. Meric Pagano, C. Vogelsang, G. Mascolo, Status of hormones and painkillers in wastewater effluents across several European states–considerations for the EU watch list concerning estradiols and diclofenac, Environ. Sci. Pollut. Res., 23 (2016) 12835–12866.
[10] K. Rehberger, E. Wernicke von Siebenthal, C. Bailey, P. Bregy, M. Fasel, E.L. Herzog, S. Neumann, H. Schmidt-Posthaus, H. Segner, Long-term exposure to low 17α-ethinylestradiol (EE2) concentrations disrupts both the reproductive and the immune system of juvenile rainbow trout, *Oncorhynchus mykiss*, Environ. Int., 142 (2020) 105836, doi: 10.1016/j.envint.2020.105836.
[11] M. Adeel, X. Song, Y. Wang, D. Francis, Y. Yang, Environmental impact of estrogens on human, animal and plant life: a critical review, Environ. Int., 99 (2017) 107–119.
[12] S. Lecomte, D. Habauzit, T.D. Charlier, F. Pakdel, Emerging estrogenic pollutants in the aquatic environment and breast cancer, Genes (Basel), 8 (2017) 229, doi: 10.3390/genes8090229.
[13] IARC, Combined Estrogen–Progestogen Contraceptives. IARC Monographs on the Evaluation of Carcinogenic Risks to Humans, International Agency for Research on Cancer, 150 cours Albert Thomas, 69372 Lyon Cedex 08, France, 2005 (2012) 100A:283–317.
[14] J. Kent, J.H. Tay, Treatment of 17α-ethinylestradiol, 4-nonylphenol, and carbamazepine in wastewater using an aerobic granular sludge sequencing batch reactor, Sci. Total Environ., 652 (2019) 1270–1278.
[15] L.L.S. Silva, J.C.S. Sales, J.C. Campos, D.M. Bila, F.V. Fonseca, Advanced oxidative processes and membrane separation for micropollutant removal from biotreated domestic wastewater, Environ. Sci. Pollut. Res., 24 (2017) 6329–6338.
[16] V. Kumar, D. Avisar, L. Prasanna V, Y. Betzalel, H. Mamane, Rapid visible-light degradation of EE2 and its estrogenicity in hospital wastewater by crystalline promoted g-C_3N_4, J. Hazard. Mater., 398 (2020) 122880, doi: 10.1016/j.jhazmat.2020.122880.
[17] X. Ma, C. Zhang, J. Deng, Y. Song, Q. Li, Y. Guo, C. Li, Simultaneous degradation of estrone, 17β-estradiol and 17α-ethinyl estradiol in an aqueous UV/H_2O_2 system, Int. J. Environ. Res. Public Health, 12 (2015) 12016–12029.
[18] A. Mohagheghian, R. Nabizadeh, A. Mesdghinia, N. Rastkari, A.H. Mahvi, M. Alimohammadi, M. Yunesian, R. Ahmadkhaniha, S. Nazmara, Distribution of estrogenic steroids in municipal wastewater treatment plants in Tehran, Iran, J. Environ. Health Sci. Eng., 12 (2014) 97, doi: 10.1186/2052-336X-12-97.
[19] R.O. Pereira, C. Postigo, M.L. de Alda, L.A. Daniel, D. Barceló, Removal of estrogens through water disinfection processes and formation of by-products, Chemosphere, 82 (2011) 789–799.
[20] D. Bila, A.F. Montalvão, D. de A. Azevedo, M. Dezotti, Estrogenic activity removal of 17β-estradiol by ozonation and identification of by-products, Chemosphere, 69 (2007) 736–746.
[21] C. Postigo, S.D. Richardson, Transformation of pharmaceuticals during oxidation/disinfection processes in drinking water treatment, J. Hazard. Mater., 279 (2014) 461–475.
[22] K. Moriyama, H. Matsufuji, M. Chino, M. Takeda, Identification and behavior of reaction products formed by chlorination of ethynylestradiol, Chemosphere, 55 (2004) 839–847.
[23] S. Hemidouche, A. Assoumani, L. Favier, A.I. Simion, C.G. Grigoras, D. Wolbert, L. Gavrila, Removal of Some Endocrine Disruptors via Adsorption on Activated Carbon, 2017 E-Health and Bioengineering Conference (EHB), IEEE, Sinaia, Romania, 2017, pp. 410–413.
[24] J. Hartmann, R. Beyer, S. Harm, Effective removal of estrogens from drinking water and wastewater by adsorption technology, Environ. Process., 1 (2014) 87–94.
[25] J. He, J. Guo, Q. Zhou, J. Yang, F. Fang, Y. Huang, Analysis of 17α-ethinylestradiol and bisphenol A adsorption on anthracite surfaces by site energy distribution, Chemosphere, 216 (2019) 59–68.
[26] L. Wang, L. Liu, Z. Zhang, B. Zhao, J. Li, B. Dong, N. Liu, 17α-Ethinylestradiol removal from water by magnetic ion exchange resin, Chin. J. Chem. Eng., 26 (2018) 864–869.
[27] J. Bedia, V. Muelas-Ramos, M. Peñas-Garzón, A. Gómez-Avilés, J.J. Rodríguez, C. Belver, A review on the synthesis

and characterization of metal–organic frameworks for photocatalytic water purification, Catalysts, 9 (2019) 52, doi: 10.3390/catal9010052.
[28] N.B. Singh, G. Nagpal, S. Agrawal, Rachna, Water purification by using adsorbents: a review, Environ. Technol. Innovation, 11 (2018) 187–240.
[29] E.M. Dias, C. Petit, Towards the use of metal–organic frameworks for water reuse: a review of the recent advances in the field of organic pollutants removal and degradation and the next steps in the field, J. Mater. Chem. A, 3 (2015) 22484–22506.
[30] C. Petit, Present and future of MOF research in the field of adsorption and molecular separation, Curr. Opin. Chem. Eng., 20 (2018) 132–142.
[31] R. Abazari, A.R. Mahjoub, J. Shariati, Synthesis of a nanostructured pillar MOF with high adsorption capacity towards antibiotics pollutants from aqueous solution, J. Hazard. Mater., 366 (2019) 439–451.
[32] M.R. Azhar, H.R. Abid, H. Sun, V. Periasamy, M.O. Tadé, S. Wang, One-pot synthesis of binary metal–organic frameworks (HKUST-1 and UiO-66) for enhanced adsorptive removal of water contaminants, J. Colloid Interface Sci., 490 (2017) 685–694.
[33] R. Liang, L. Shen, F. Jing, N. Qin, L. Wu, Preparation of MIL-53(Fe)-reduced graphene oxide nanocomposites by a simple self-assembly strategy for increasing interfacial contact: efficient visible-light photocatalysts, ACS Appl. Mater. Interfaces, 7 (2015) 9507–9515.
[34] Q. Sun, M. Liu, K. Li, Y. Zuo, Y. Han, J. Wang, C. Song, G. Zhang, X. Guo, Facile synthesis of Fe-containing metal–organic frameworks as highly efficient catalysts for degradation of phenol at neutral pH and ambient temperature, Cryst. Eng. Comm, 17 (2015) 7160–7168.
[35] X. Liu, Y. Zhou, J. Zhang, L. Tang, L. Luo, G. Zeng, Iron containing metal–organic frameworks: structure, synthesis, and applications in environmental remediation, ACS Appl. Mater. Interfaces, 9 (2017) 20255–20275.
[36] N.M. Mahmoodi, J. Abdi, Nanoporous metal–organic framework (MOF-199): synthesis, characterization and photocatalytic degradation of Basic Blue 41, Microchem. J., 144 (2019) 436–442.
[37] M.A. Ghasemzadeh, B. Mirhosseini-Eshkevari, M.H. Abdollahi-Basir, MIL-53(Fe) metal–organic frameworks (MOFs) as an efficient and reusable catalyst for the one-pot four-component synthesis of pyrano[2,3-c]-pyrazoles, Appl. Organomet. Chem., 33 (2019) e4679, doi: 10.1002/aoc.4679.
[38] P. Gautam, T. Purvis, Method development and validation of stability indicating RP-HPLC method for the determination of female hormones in hormone concentrates creams, Pharm. Anal. Chem., 3 (2017) 1000120, doi: 10.4172/2471-2698.1000120.
[39] B.M. Peake, R. Braund, A.Y.C. Tong, L.A. Tremblay, Detection and Presence of Pharmaceuticals in the Environment, In: The Life-Cycle of Pharmaceuticals in the Environment, Woodhead Publishing which is an imprint of Elsevier, 80 High Street, Sawston, Cambridge, CB22 3HJ, UK, 2016, pp. 77–107.
[40] C.M. Navarathna, N.B. Dewage, A.G. Karunanayake, E.L. Farmer, F. Perez, E.B. Hassan, T.E. Mlsna, C.U. Pittman Jr., Rhodamine B adsorptive removal and photocatalytic degradation on MIL-53-Fe MOF/magnetic magnetite/biochar composites, J. Inorg. Organomet. Polym. Mater., 30 (2020) 214–229.
[41] Z. Zhang, X. Li, B. Liu, Q. Zhao, G. Chen, Hexagonal microspindle of NH_2-MIL-101(Fe) metal–organic frameworks with visible-light-induced photocatalytic activity for the degradation of toluene, RSC Adv., 6 (2016) 4289–4295.
[42] Q. Xie, Y. Li, Z. Lv, H. Zhou, X. Yang, J. Chen, H. Guo, Effective adsorption and removal of phosphate from aqueous solutions and eutrophic water by Fe-based MOFs of MIL-101, Sci. Rep., 7 (2017) 3316, doi: 10.1038/s41598-017-03526-x.
[43] U.B. Simsek, C. Geçgel, M. Turabik, Different Iron Based Metal–Organic Frameworks Synthesis, Characterization and Using for Amoxicillin Removal from Aqueous Solutions, 2nd International Mediterranean Science and Engineering Congress (IMSEC 2017), Adana, 2017, pp. 1–7.
[44] E. Yılmaz, E. Sert, F.S. Atalay, Synthesis, characterization of a metal–organic framework: MIL-53(Fe) and adsorption mechanisms of methyl red onto MIL-53(Fe), J. Taiwan Inst. Chem. Eng., 65 (2016) 323–330.
[45] S.G. Herawan, M.S. Hadi, Md. R. Ayob, A. Putra, Characterization of activated carbons from oil-palm shell by CO_2 activation with no holding carbonization temperature, Sci. World J., 2013 (2013) 624865, doi: 10.1155/2013/624865.
[46] L. Jiang, Y. Liu, G. Zeng, S. Liu, X. Hu, L. Zhou, X. Tan, N. Liu, M. Li, J. Wen, Adsorption of estrogen contaminants (17β-estradiol and 17α-ethynylestradiol) by graphene nanosheets from water: effects of graphene characteristics and solution chemistry, Chem. Eng. J., 339 (2018) 296–302.
[47] B.M. Jun, H.S. Hwang, J. Heo, J. Han, M. Jang, J. Sohn, C.M. Park, Y. Yoon, Removal of selected endocrine-disrupting compounds using Al-based metal–organic framework: performance and mechanism of competitive adsorption, J. Ind. Eng. Chem., 79 (2019) 345–352.
[48] Z. Luo, H. Li, Y. Yang, H. Lin, Z. Yang, Adsorption of 17α-ethinylestradiol from aqueous solution onto a reduced graphene oxide-magnetic composite, J. Taiwan Inst. Chem. Eng., 80 (2017) 797–804.
[49] L. Mita, M. Forte, A. Rossi, C. Adamo, S. Rossi, D.G. Mita, M. Guida, M. Portaccio, T. Godievargova, I. Yavour, M. Samir, M. Eldin, Removal of 17-α ethinylestradiol from water systems by adsorption on polyacrylonitrile beads: isotherm and kinetics studies, Ann. Environ. Sci. Toxicol., 2 (2017) 48–58.
[50] S. Rahman, A. Arami-Niya, X. Yang, G. Xiao, G. (Kevin) Li, E.F. May, Temperature dependence of adsorption hysteresis in flexible metal–organic frameworks, Commun. Chem., 3 (2020) 186, doi: 10.1038/s42004-020-00429-3.
[51] L.A. Al-Khateeb, A.Y. Obaid, N.A. Asiri, M. Abdel Salam, Adsorption behavior of estrogenic compounds on carbon nanotubes from aqueous solutions: kinetic and thermodynamic studies, J. Ind. Eng. Chem., 20 (2014) 916–924.
[52] X. Wang, Z. Liu, Z. Ying, M. Huo, W. Yang, Adsorption of trace estrogens in ultrapure and wastewater treatment plant effluent by magnetic graphene oxide, Int. J. Environ. Res. Public Health, 15 (2018) 1454, doi: 10.3390/ijerph15071454.